Fully differential study of dissociative single capture and Coulomb explosion through double capture in $p + H_2$ collisions

B. R. Lamichhane,[1] A. Hasan,[1,2] T. Arthanayaka,[1] M. Dhital,[1] K. Koirala,[1] T. Voss,[1] R. A. Lomsadze,[1,3] and M. Schulz[1]

[1]*Department of Physics and LAMOR, Missouri University of Science & Technology, Rolla, Missouri 65409, USA*
[2]*Department of Physics, UAE University, P.O. Box 15551, Al Ain, Abu Dhabi, UAE*
[3]*Physics Department, Tbilisi State University, Tbilisi 0179, Georgia*

We have measured fully differential cross sections for dissociative single capture and Coulomb explosion through double capture in 75 keV $p + H_2$ collisions. Data were analyzed for fixed kinetic energy releases and molecular orientations as a function of scattering angle. Two-center interference was identified for dissociative single capture. The interference pattern is not inconsistent with the symmetry of the dissociative electronic state affecting the phase angle of the interference term. No clear signatures of single-center interference were observed for either process. For double capture at most only a very weak two-center interference structure was found. This very small (or zero) visibility can probably be attributed to a convolution of two independent scatterings of the projectile with the two electrons yielding the measured scattering angle.

I. INTRODUCTION

The basic interest underlying most research on atomic collisions is to advance our understanding of the few-body dynamics of processes occurring in simple atomic systems [e.g., 1–4]. The fundamental difficulty is that the Schrödinger equation is not analytically solvable for more than two mutually interacting particles. Therefore, theory has to resort to elaborate numeric modelling efforts. The assumptions and approximations entering in these models have to be tested by detailed experimental data.

Experimental data which exhibit interference structures are particularly suitable to test theoretical models because the interference pattern depends sensitively on the details of the few-body dynamics. An example is molecular two-center interference, which has been observed in numerous experimental studies and predicted by theory for charged particles colliding with diatomic molecules [e.g., 5–20]. There, the diffracted projectile waves originating from the two atomic centers interfere with each other. However, the identification of an interference pattern can be rather challenging. Experiments which integrate over certain kinematic parameters effectively average the cross sections over the phase angle so that the interference structure may be partly or completely "smeared out." If differential cross sections are analyzed as a function of scattering angle, the interference pattern is usually superimposed on a steep dependence of the incoherent cross sections on the scattering angle, which can also significantly reduce the visibility of an oscillating pattern.

Pronounced interference structures were found when the momenta of all collision fragments were determined with good resolution [12]. One approach to identify an interference pattern even when it is not or barely visible in the cross sections is to normalize the cross sections to those one would obtain without the interference term, to which we refer as the incoherent cross section $d\sigma_{inc}$. In analogy to classical optics the cross section including the interference term I (coherent cross section) can be expressed as $d\sigma_{coh} = d\sigma_{inc}I$, so that I is given by the coherent to incoherent cross section ratio R [7–10,13,15,16]. The difficulty with this approach is that until

recently it was not clear how $d\sigma_{inc}$ could be experimentally determined. Therefore, $d\sigma_{inc}$ was often approximated as the cross section for two separate H atoms or a He target [7–10,13,15,16]. In R even small differences between the real and approximated incoherent cross sections can lead to artificial structures, which could be misinterpreted as interference structures.

A few years ago, we demonstrated that $d\sigma_{inc}$ can be experimentally determined with high accuracy by manipulating the projectile coherence properties by placing a collimating slit in front of the target [17]. If a slit of fixed width is placed at a large distance from the target, the local collimation angle subtended by the slit at the target position corresponds to a small momentum spread of the incoming wave, which, in turn, corresponds to a large coherence length Δr. The incoming projectile wave can then coherently illuminate both atomic scattering centers of the molecule simultaneously and interference between the diffracted waves from both centers is observable. Likewise, a small slit distance results in a large local collimation angle, i.e., a large momentum spread, so that the coherence length is not sufficiently large for both atomic centers to be simultaneously illuminated by the projectile wave. In this case no interference is observed. Therefore, the interference term can be accurately determined as the ratio between the cross sections measured for a large and a small slit distance.

The interpretation offered in Ref. [17] was challenged by Feagin and Hargreaves [21], who argued that the differences between the cross sections measured for the large and small slit distances were merely due to differences in the beam divergence. However, this assertion was rebutted by Sharma *et al.* [22], who demonstrated that there were no noticeable differences in the beam divergence for the two slit distances. Later, resolution-independent coherence effects were reported for various processes and targets for projectiles with relatively small speed and large perturbation parameters η (projectile charge to speed ratio) [19,20,23,24; for a review see Ref. [25]]. Two experimental studies also reported coherence effects for large projectile speeds and atomic targets [26,27], while no such effects were observed [28] for a similar collisions

system as investigated in Ref. [26]. However, the smallest coherence length realized in Ref. [28] was about three orders of magnitude larger than in Ref. [26] and larger than the size of the target atom.[1] Therefore, no significant coherence effects were expected, as also confirmed by a recent theoretical study [29]. Nevertheless, at small η further experimental and theoretical studies are needed to confirm or disprove such coherence effects.

In contrast, at large η the extensive literature on coherence effects strongly suggests that indeed such effects can play an important role in ion–atom/molecule collisions. Here, research is now entering the next phase in which coherence effects are used as a tool to study the few-body dynamics in more detail. To this end we recently reported measurements of fully differential cross sections (FDCS) for single capture accompanied by vibrational dissociation in $p + H_2$ collisions for various molecular orientations as a function of scattering angle [30]. In this process, the second electron stays in the ground state and dissociation proceeds through excitation of the nuclear motion to a vibrational continuum state. By analyzing the coherent to incoherent FDCS ratios we were able to identify single-center and two-center interference simultaneously in the same data set. The former, in which different impact parameters leading to the same scattering angle interfere with each other, can also occur for atomic targets [20,24,25,31]. More importantly, an unexpected shift of π was observed in the phase angle for two-center interference. Such a phase shift was also found for $H_2^+ + He$ collisions and was explained by a switch in the symmetry of the final compared to the initial electronic state [12,16]. However, no such switch in symmetry occurs in vibrational dissociation studied in Ref. [30]. Furthermore, the interference patterns observed for double capture [11] and dissociative ionization by electron impact [15] cannot be explained by the electronic symmetry either. These data suggest that there are other factors apart from the electronic symmetry which can lead to (or counteract) a phase shift. This, in turn, implies that the phase angle, and therefore the few-body reaction dynamics, is not fully understood yet.

Here, we report measured FDCS for another dissociative single capture channel, namely capture accompanied by excitation of the second electron to a repulsive electronic state, as well as for Coulomb explosion induced by double capture. We focus on FDCS for a molecular orientation parallel to the transverse component of the momentum transfer **q** (difference between the initial and final projectile momentum). Data were obtained for a kinetic energy release (KER) for which two electronic states of opposite symmetry predominantly contribute to dissociation.

II. EXPERIMENT

The experiment was performed at Missouri University of Science & Technology. The experimental set-up is essentially the same as the one used in Ref. [18] and is shown in Fig. 1. A proton beam was generated with a hot cathode ion source and
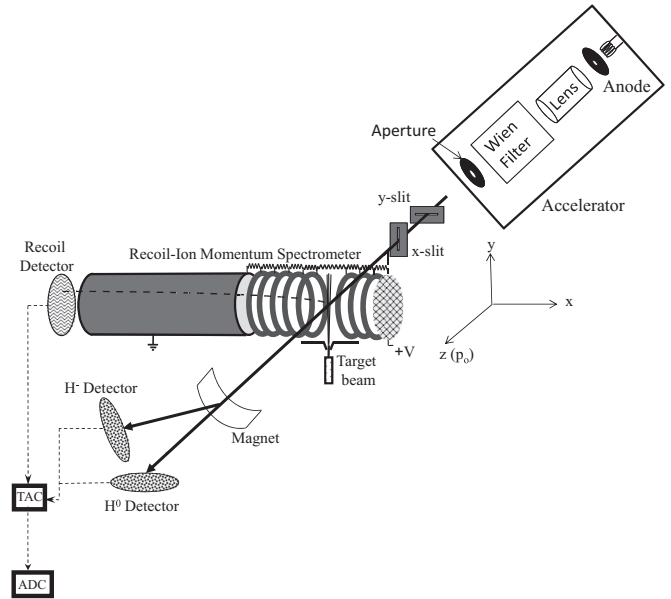

FIG. 1. Schematic diagram of the experimental set-up.

accelerated to an energy of 75 keV. The beam was collimated by a vertical slit (x-slit), placed at a distance from the target of $L_1 = 6.5$ cm, and a horizontal slit (y slit), placed at a distance $L_2 = 50$ cm, both with a width of 150 μm. These slit distances correspond to transverse coherence lengths of $\Delta x = 0.43$ a.u. in the x direction and $\Delta y = 3.3$ a.u. in the y direction. However, in the x direction the coherence properties are not determined by the collimating slit, but rather by an aperture at the end of the accelerator terminal so that the smaller coherence length is about $\Delta x = 1.0$ a.u. [19].

The collimated projectile beam was then crossed with a very cold ($T \approx 1$–2 K)H_2 beam from a supersonic jet propagating in the y direction. The molecular proton fragments produced in the collision were extracted by a uniform electric field of 250 (for dissociative single capture) to 350 V/cm (for double capture) pointing in the $-x$ direction and guided onto a two-dimensional position-sensitive channel-plate detector. For dissociative single capture at these field strengths, all proton fragments with energies up to 7.5 eV (i.e., KER = 15 eV) hit the detector. For the double capture experiment, the recoil-ion spectrometer axis was slightly tilted and the detector slightly moved up compared to the settings for dissociative single capture such that the fragments with small momenta in the plane of the detector were steered from the center towards the lower right corner of the detector. The data were then later analyzed only for the upper left quadrant relative to the position corresponding to a zero momentum. In this way, FDCS for double capture could be obtained without suppressing certain orientations relative to others for KER values of up to about 30 eV.

After the target region the projectile beam was charge-state analyzed by a switching magnet. A second two-dimensional position-sensitive channel-plate detector was positioned either at 0° relative to the initial beam direction, so that the neutralized projectiles were detected (dissociative single capture), or at 45°, so that H⁻ projectiles were detected (double capture). The detector was set in coincidence with the molecular fragment

---

[1]The coherence length reported in Ref. [28] was calculated incorrectly and was too small by about 65%.

detector. From the coincidence time the time of flight of the molecular proton fragments were determined and thereby the momentum component in the direction of the extraction field. The momentum components in the y and z directions were obtained from the position information. From the momentum components the molecular orientation and the KER value were calculated. At such a large extraction field the momentum resolution is primarily determined by the size of the interaction volume and by the position and time resolution of the detector [32]. Furthermore, it depends on the momentum itself. For $p = 35$ a.u. it was about 2 a.u. full width at half maximum (FWHM) for all components resulting in a KER resolution of about 3 eV FWHM. The polar and azimuthal angular resolution in the molecular orientation was about 10° FWHM.

From the position information of the projectile detector the polar and azimuthal scattering angles were determined. The FDCS for coherent and incoherent projectiles were obtained simultaneously, under otherwise identical experimental conditions, by setting conditions on the azimuthal angle to select scattering in the x direction (incoherent) or in the y direction (coherent). The resolution in the polar angle was about 0.15 mrad FWHM and in the azimuthal angle it was very small (3° FWHM) compared to the entire 360° range contributing to all dissociation events. However, to obtain the FDCS with sufficient statistics the condition on the azimuthal angle had a width of $\pm 15°$.

III. DATA ANALYSIS

In Fig. 2, we show coincidence time spectra for dissociative single capture (top panel) and double capture (bottom panel). In the case of dissociative capture, a pronounced triple peak structure is visible. A similar shape of the time spectrum was also observed for dissociative ionization in fast $p + H_2$ collisions [33]. The center peak reflects events in which the molecular proton fragment has a small momentum in the direction of the extraction field. This can be realized either by a small KER value, occurring in dissociation through vibrational excitation [30], or by a molecular orientation in the plane perpendicular to the extraction field. The left maximum is due to fragments which gained a large momentum towards the detector in the dissociation and the right maximum those in which the fragments gained a large momentum away from the detector. In the time spectrum for double capture the center peak is missing. This can be understood by the fact that here Coulomb explosion, for which small KER values are not possible, is the only fragmentation channel. Apparently, the contributions from molecules oriented in the plane perpendicular to the extraction field are not large enough to lead to a resolved center peak structure.

In Fig. 3, we show KER spectra for three different cases. The closed circles represent dissociative capture measured with a small extraction field of only 50 V/cm. In this case all fragments from molecules oriented in the plane perpendicular to the extraction field with a momentum larger than 14 a.u. (corresponding to KER = 3 eV) miss the detector. As a result, large KER values, resulting from electronic transitions to repulsive states, are strongly suppressed. The spectrum is dominated by small KER values representing dissociation by vibrational excitation, for which data were reported previously [30]. The
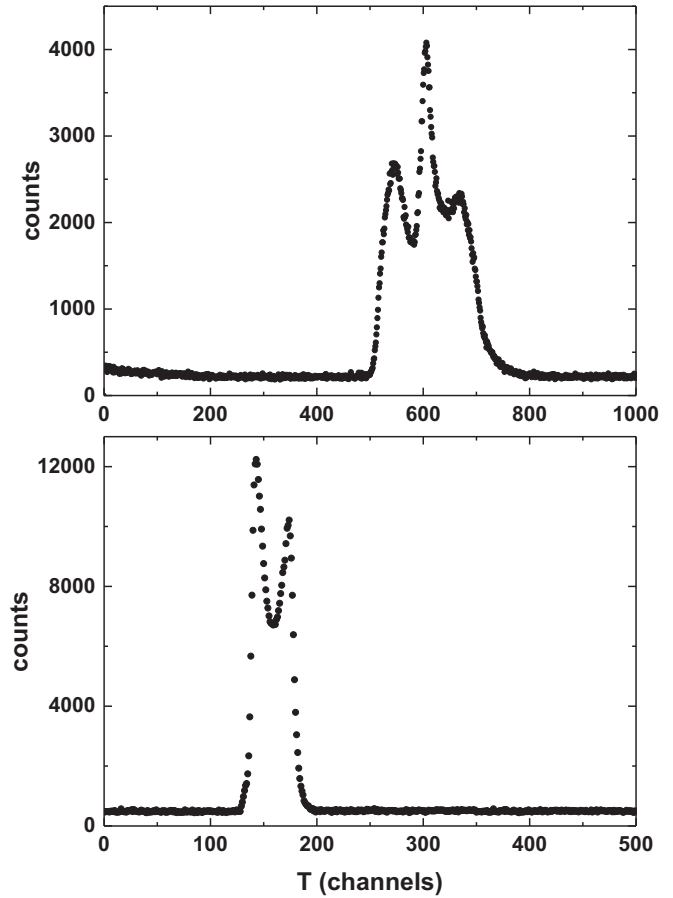

FIG. 2. Time spectrum of coincidences between neutralized projectiles and molecular proton fragments (top panel) and H^- projectiles and molecular proton fragments (bottom panel).

open circles represent dissociative single capture measured with an extraction field of 250 V/cm. Now, all fragments with energies up to 7.5 eV (KER = 15 eV), regardless of
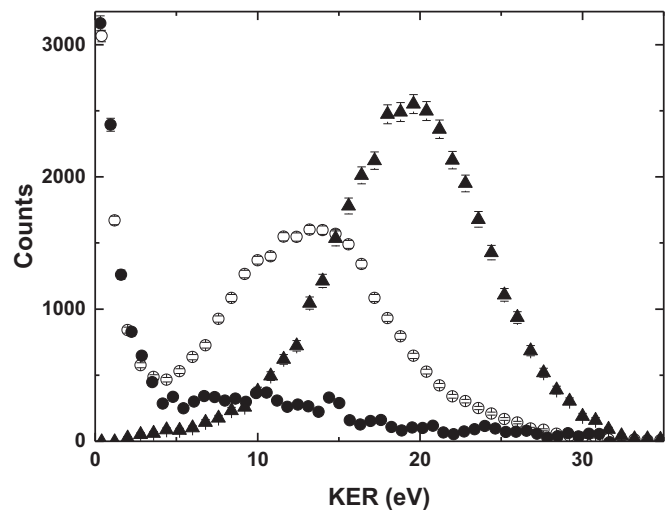

FIG. 3. Kinetic energy release (KER) spectrum coincident with H° projectiles (open and closed circles) and with H^- projectiles (solid triangles). The open (closed) circles were recorded with a large (small) recoil-ion extraction voltage.

orientation, hit the detector. As a result, a pronounced and separate peak structure at 13 eV is observed. Finally, the closed triangles represent double capture measured with an extraction field of 350 V/cm. Now, the small KER component, which is very pronounced for dissociative single capture, is completely absent. Rather, only a single peak structure with the centroid at 19.5 eV, corresponding to the potential energy of the two protons at the equilibrium distance of H_2, is observed.

Earlier, we reported FDCS for a condition on KER $= 0$ to 2 eV, i.e., for electronic ground state dissociation through vibrational excitation [30]. Here, we analyzed FDCS for dissociative single capture for a condition KER $= 5$–12 eV. In this region contributions to dissociation come mostly from the $2p\pi_u$ and $2s\sigma_g$ states and, to a much lesser extent, from the $2p\sigma_u$ state of H_2^+ [34]. In the case of double capture Coulomb explosion is the only fragmentation channel. Here, the KER value unambiguously determines the internuclear separation D at the instance of the collision as D $= 1/$KER (in a.u.). Data were analyzed for KER regions of 13–18 eV, 18–22 eV, and 22–27 eV.

In addition to the KER value conditions were also set on the molecular orientation and on the azimuthal projectile scattering angle. FDCS will be presented for two molecular orientations, which are illustrated in Fig. 4. Both of them are perpendicular to the projectile beam axis (i.e., the polar molecular angle is centered on $\theta_m = 0°$). One of them (top panel of Fig. 4) is perpendicular also to the transverse component of the momentum transfer q_{tr} (i.e. $\varphi_m = 90°$) while the second (bottom panel of Fig. 4) is parallel to q_{tr} (i.e., $\varphi_m = 0°$). For simplicity, in the following we refer to these orientations as the perpendicular and parallel orientation, respectively. The corresponding conditions in the azimuthal and polar angles of the detected molecular proton fragments had a width of $\Delta\theta_m$ and $\Delta\varphi_m = \pm 15°$.

To select coherent and incoherent incoming projectiles a condition was also set on the azimuthal projectile scattering angle $\varphi_p = 0° \pm 15°$ (scattering in x direction, incoherent) and $\varphi_p = 90° \pm 15°$ (scattering in y direction, coherent). For each KER value four fully differential spectra were generated as a function of the polar projectile scattering angle θ_p:(1) $\varphi_p = 0°$ and $\varphi_m = 0°$ (incoherent projectiles, parallel orientation); (2) $\varphi_p = 0°$ and $\varphi_m = 90°$ (incoherent projectiles, perpendicular orientation); (3) $\varphi_p = 90°$ and $\varphi_m = 0°$ (coherent projectiles, perpendicular orientation); (4) $\varphi_p = 90°$ and $\varphi_m = 90°$ (coherent projectiles, parallel orientation).

IV. RESULTS AND DISCUSSION

In Fig. 5 FDCS are plotted for dissociative single capture for the perpendicular orientation and KER $= 5$–12 eV as a function of θ_p. The open symbols represent the FDCS for the incoherent projectiles and the closed symbols those for the coherent projectiles. Within the statistical fluctuations no significant differences between the coherent and incoherent data can be discerned. The phase angle for two-center interference is determined by the dot product between the internuclear separation vector and the recoil-ion momentum, which for capture is equal to **q**. For the perpendicular orientation this dot product is constant at zero for all θ_p so that no differences between the coherent and incoherent
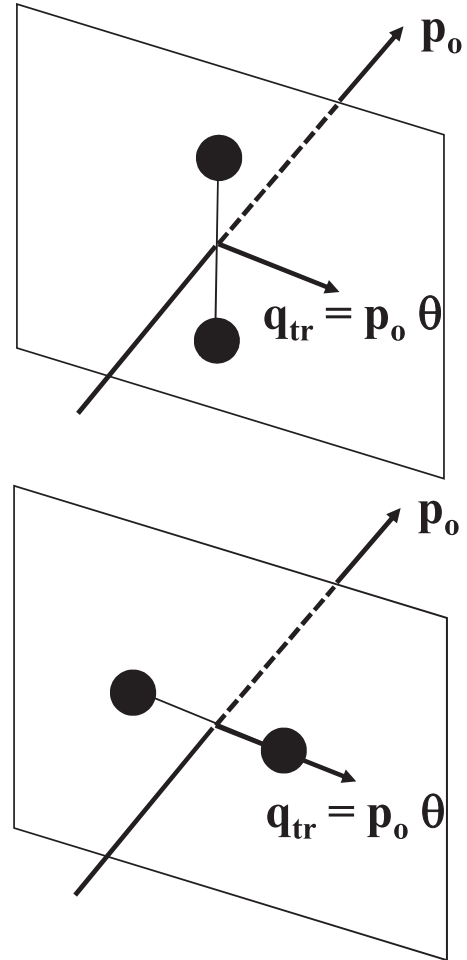

FIG. 4. Illustration of the two molecular orientations for which fully differential cross sections were analyzed. The top panel shows the perpendicular and the bottom panel the parallel orientation (relative to the transverse component of the momentum transfer).

FDCS due to two-center interference are expected. However, for KER $= 0$–2 eV, i.e., for dissociative capture through vibrational excitation, we found significant differences caused by single-center interference [30].

One possible explanation for the apparent absence of single-center interference in the present data is that dissociation leading to a large KER requires a two-electron process (capture of one electron and excitation of the second electron to an anti-binding state). At the relatively large η for this collision system the transitions of both electrons are predominantly caused by two independent interactions with the projectile. Therefore, the measured total scattering angle is the result of a convolution of the deflections of the projectile in these two steps. This convolution is reflected in the scattering angle dependence of the interference term and thus can lead to a loss of visibility.

In Fig. 6 the FDCS are shown for the parallel orientation under otherwise identical kinematic conditions as in Fig. 5. For this orientation we observe some differences between the coherent and incoherent data. Between approximately 0.4 and 1.2 mrad the coherent FDCS lie systematically below the incoherent FDCS, while between 1.3 and 2.1 mrad they
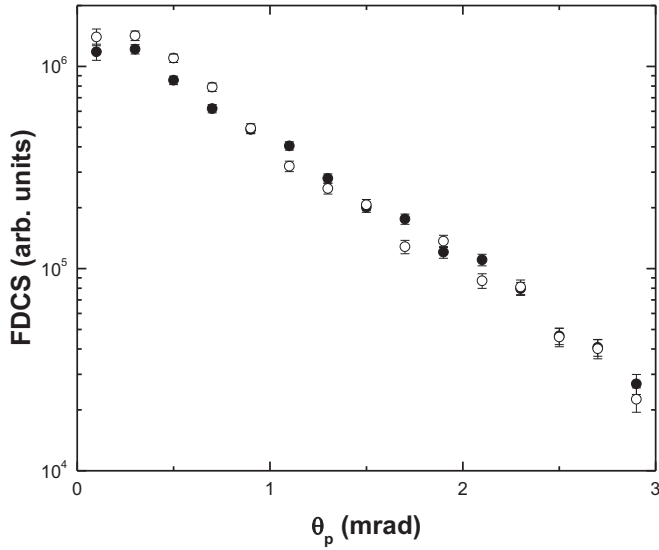
FIG. 5. Fully differential cross sections (FDCS) for dissociative capture leading to KER = 5 − 12 eV and a molecular orientation perpendicular to both the initial projectile beam axis and the transverse component of the momentum transfer as a function of scattering angle. The open (closed) symbols represent the data taken with an incoherent (coherent) projectile beam.

FIG. 6. Same as Fig. 5, but molecular orientation is parallel to the transverse component of the momentum transfer.

FIG. 7. Ratios between the FDCS for coherent and incoherent projectiles from Fig. 6 as a function of scattering angle. Dashed curve, two-center interference term expected for a gerade dissociative state; dotted curve, two-center interference term expected for an ungerade dissociative state; solid curve, sum of the dashed and dotted curves with weight factors of f and 1 - f for the geared and ungerade states, respectively. For f, see text.

are systematically larger. These differences are more clearly visible in the coherent to incoherent FDCS ratios $R_\parallel$, which are plotted in Fig. 7, in terms of a departure from $R_\parallel = 1$, especially in the maximum seen at about 1.7 mrad (and possibly a shallow minimum at 0.9 mrad). While this structure is statistically significant, it is not as pronounced as in the case of vibrational dissociation and the interference extrema occur at different angles [30]. The reason that it is visible at all in spite of the underlying double projectile scattering, in contrast to single-center interference, is probably that for single scattering (like in, e.g., vibrational dissociation) two-center interference is significantly more pronounced than single-center interference [30]. A two-center interference
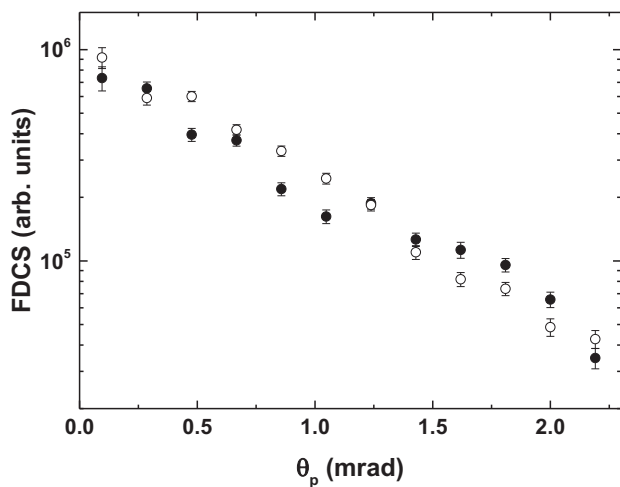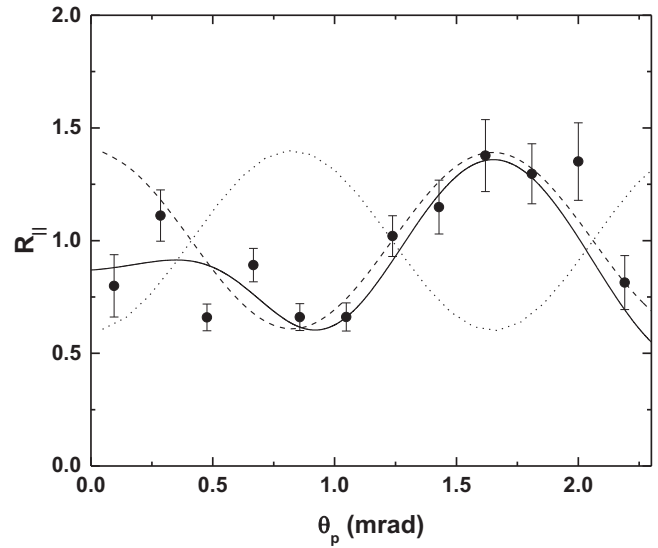
structure thus has a better chance of partly surviving the convolution over two scatterings.

Given the argument that a switch in the symmetry of the electronic state should lead to a π phase shift in the two-center interference term one might not necessarily had expected a pronounced interference structure in the selected KER regime. The total interference term is a sum of those obtained for the $2p\pi_u$ state, for which a π shift would be expected, and the $2s\sigma_g$ state, for which no phase shift would be expected. Thus, if the contributions from both states would be exactly identical this sum should exhibit no dependence at all on θ_p. However, for electron impact, at the same projectile speed as in our study, Edwards and Zheng demonstrated that the relative cross sections for excitation to the $2p\pi_u$ and $2s\sigma_g$ states sensitively depend on the angle θ_{mq} between the molecular axis and **q** [35], which is illustrated in the top panel Fig. 8. For small θ_{mq} the $2s\sigma_g$ state is predominantly populated and for large θ_{mq} contributions from the $2p\pi_u$ state are larger.

For the parallel orientation the molecular axis vector **D** and **q** lie in the same plane and the polar molecular angle is fixed at $\theta_m = 90°$. Therefore, the angle between **q** and the projectile beam axis θ_p and θ_{mq} always add up to 90° (see Fig. 8). Furthermore, θ_p is given by

$$\theta_q = \text{tg}^{-1}(q_{tr}/q_z), \quad (1)$$

where $q_{tr} = p_o \sin(\theta_p)$. Therefore, for this geometry θ_{mq} is unambiguously determined by θ_p as

$$\theta_{mq} = \pi/2 - \text{tg}^{-1}(p_o \sin(\theta_p)/q_z); \quad (2)$$

i.e., large θ_p correspond to small θ_{mq} and vice versa. Here, the longitudinal component of **q** is given by $q_z = -Q/v_p - v_p/2$, where Q is the Q value of the reaction and v_p is the projectile
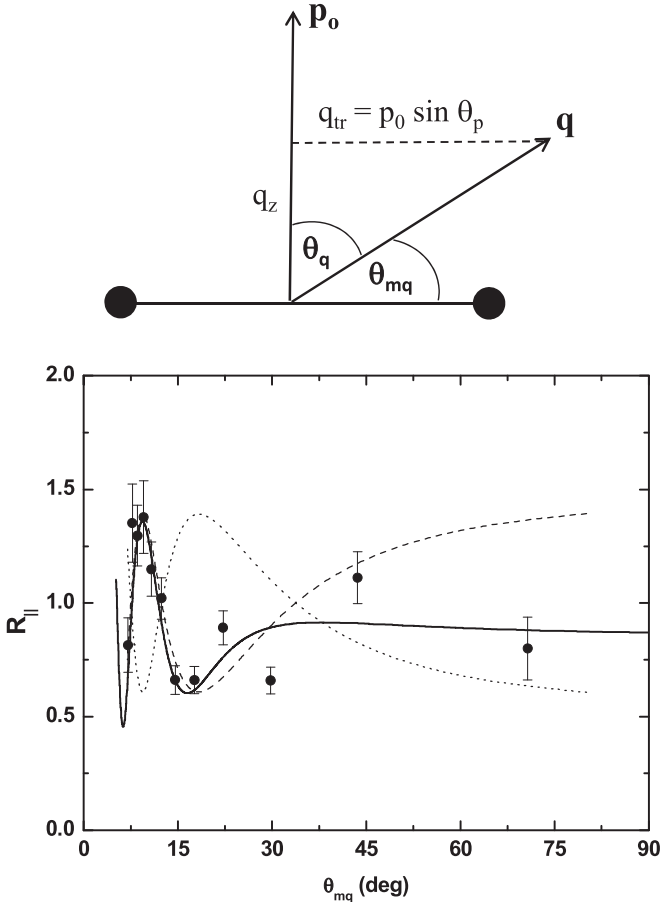
FIG. 8. Top panel: illustration of the angle θ_q enclosed by the momentum transfer **q** and the projectile beam axis and of the angle θ_{mq} enclosed by the molecular axis and **q**. Bottom panel: ratios of Fig. 7 plotted as a function of the angle between the molecular axis and the momentum transfer vector θ_{mq} calculated with Eq. (2). Curves: same as in Fig. 7.

speed. The data of Fig. 7 are replotted in the bottom panel of Fig. 8 as a function of θ_{mq}. In this presentation, a sharp peak structure is seen at about $8°$. If the dependence of the relative $2s\sigma_g$ to $2p\pi_u$ population on θ_{mq} is similar as in Ref. [35] then this peak structure should be caused by two-center interference without phase shift expected for the $2s\sigma_g$ state. The interference term expected for a gerade state is given by

$$I_2 = 1 + \alpha\cos(\mathbf{q} \cdot \mathbf{D}), \qquad (3)$$

where α, which we call the visibility factor, describes to what extent the interference is "washed out" due to incomplete coherence (even at the large slit distance) and experimental resolution. I_2 calculated for $\alpha = 0.4$, which is plotted as the dashed curve in Figs. 7 and 8, is in very good agreement with the experimental data for $\theta_{mq} < 20°$ and $\theta_p > 0.8$ mrad, respectively. At the same time the same interference term for ungerade states (dotted curve) is in poor agreement with the data. For larger θ_{mq} (smaller θ_p) we have only four data points with relatively large statistical fluctuations so that no conclusions can be drawn. The solid curve represents a sum of the interference terms for the gerade and ungerade
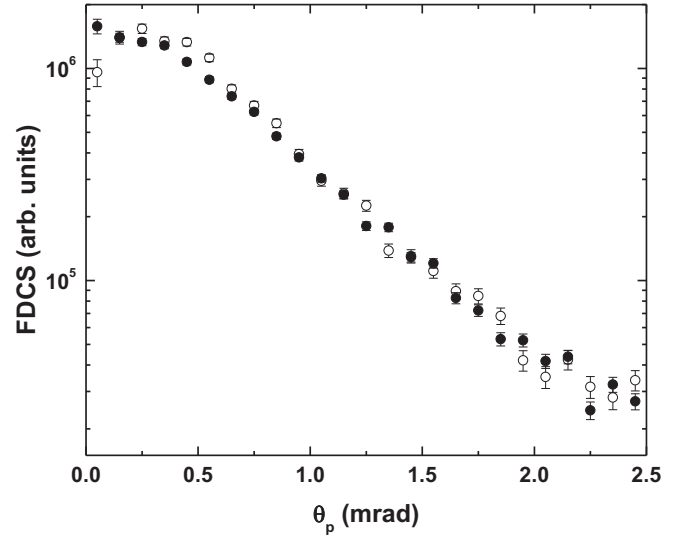

FIG. 9. Same as Fig. 5 for double capture, but integrated over all KER.

states, where each state was given a weight of f and 1 - f, respectively. f was obtained by fitting a Woods-Saxon distribution as a function of θ_{mq} to the relative $2s\sigma_g$ to $2p\pi_u$ populations given by Edwards and Zheng [35]. Overall, this combined interference term appears to be consistent with the experimental data in the entire angular range thus supporting the interpretation that a switch in the symmetry of the electronic state has to be compensated by a phase shift in the diffracted projectile wave.

One question that still needs to be addressed is why the interference structure is significantly less pronounced than for vibrational dissociation. In addition to the aforementioned convolution over the two projectile scatterings off both electrons two other factors may contribute to a loss of visibility of the interference structure. First, the two interference terms for the gerade and ungerade states mutually weaken the structures of the separate terms because they are phase-shifted relative to each other. However, the comparison between the dashed curves and the experimental data in Fig. 7 shows that only for $\theta_p < 0.5$ mrad this has a significant effect. Second, the width of the condition on the KER value corresponds to a range of internuclear distances contributing to the FDCS. As a result, the phase angle in the interference term, **q•D**, is afflicted with some uncertainty. This factor becomes increasingly important with increasing θ_p. In the region of the interference maximum θ_{tr} is about 5 a.u. Thus, a spread in D of 0.2 a.u. can cause a spread in the phase angle of about $\pi/3$, which could lead to a significant loss of visibility.

Further information as to which of these three factors is mostly responsible for the damping of the interference structure we obtained from the data on double capture. The cross-section differential in the projectile and molecular solid angles is plotted in Figs. 9 and 10 for the perpendicular and parallel orientation, respectively, as a function of θ_p. Hardly any differences between the coherent and incoherent cross sections are discernable for either orientation; i.e., neither single- nor two-center interference can be clearly identified in the data. A fit of I_2 (with and without π phase shift)
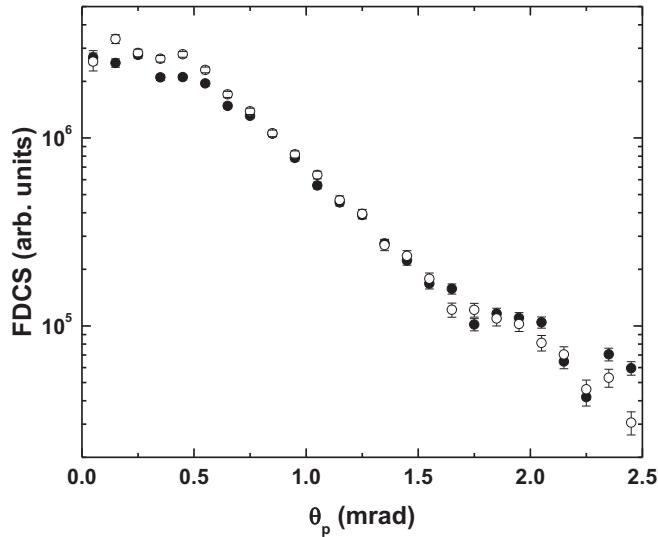
FIG. 10. Same as Fig. 6 for double capture, but integrated over all KER.

to the coherent to incoherent FDCS ratios for the parallel orientation suggests an upper limit of the visibility factor α of 0.2. Furthermore, if any interference structure is present at all (i.e., if $\alpha > 0$) then the fit slightly favors the interference term without a phase shift.

If the (near-) absence of two-center interference for the parallel orientation is primarily caused by the integration over all KER (i.e., by the spread in D) then one would expect that setting a condition on KER would lead to a visible interference pattern. For two reasons such a condition should have a more sensitive effect on the visibility than for dissociative single capture. First, since for double capture Coulomb explosion is the only fragmentation channel D is unambiguously determined by the KER value. Furthermore, since both electrons are removed from the molecule by the double capture process the relation between D and KER is not afflicted with any uncertainties introduced by screening. Second, for double capture we achieved better statistics than for dissociative capture and as a result conditions on KER could be set with narrower windows.

In Fig. 11 FDCS for the parallel orientation are shown for KER ranges of 13–18 eV (top panel), 18–22 eV (center panel), and 22–27 eV (bottom panel). Here, too, no substantial differences between the coherent and incoherent data are observed for any of the KER ranges. This suggests that the (near-) absence of interference structures is not primarily caused by any uncertainty in D. Rather, multiple scattering of the projectile from the target seems to be mostly responsible for a "washing out" of the interference pattern. In this case, a pronounced interference structure should be observable for much faster projectiles. In this regime double capture predominantly occurs through a correlated process, i.e., a single-scattering process. Indeed, pronounced interference structures were observed in double capture cross sections as a function of the molecular orientation in fast $He^{2+} + H_2$ collisions [36].

It seems plausible that the reduced visibility of the interference structure for dissociative capture, compared to vibrational
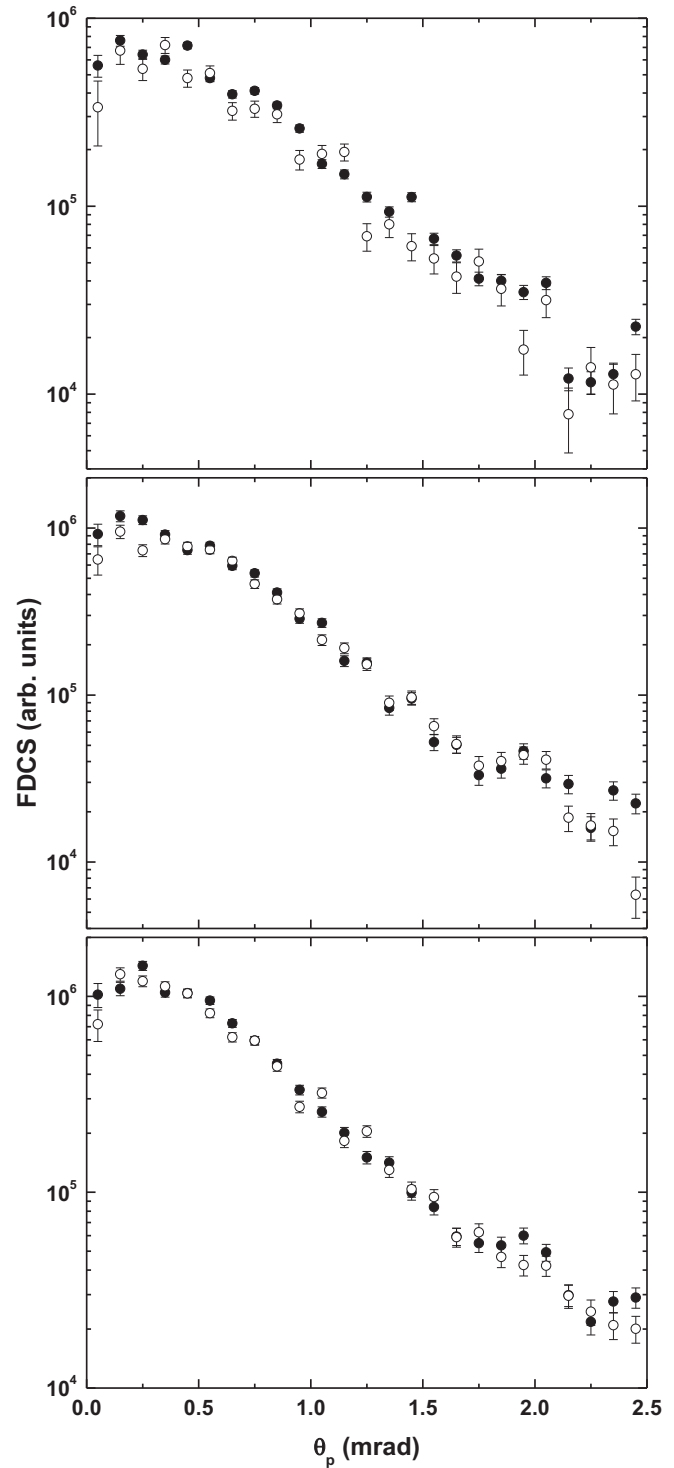

FIG. 11. Same as Fig. 10, but KER fixed at 13 to 18 eV (top panel), 18–22 eV (center panel), and 22–27 eV (bottom panel).

dissociation, is mostly due to multiple scattering as well. Then, the three data sets on molecular fragmentation, for vibrational dissociation (published in Ref. [30]), for dissociation by an electronic transition to a repulsive state, and for double capture, exhibit a systematic trend: the visibility seems to be the smaller the more violent (on average) the collision between the projectile and the target. More specifically, the

visibility maximizes for the one-electron process vibrational dissociation, presumably favoring relatively distant collisions, and minimizes for double capture, presumably the process which is most selective on close collisions.

V. CONCLUSIONS

We have measured fully differential cross sections for dissociative single capture through excitation of the second electron to a repulsive state and for double capture leading to Coulomb explosion. Data were obtained for molecular orientations perpendicular and parallel to the transverse component of the momentum transfer, respectively. For neither process did we observe any signature of single-center interference effects, which are quite pronounced in the FDCS for vibrational dissociation for the perpendicular orientation [30]. Two-center interference structures were found in the FDCS for the parallel orientation for dissociative single capture. Here, contrary to vibrational dissociation, no phase shift of π in the interference term was found. Since the data are dominated by electron excitation to a gerade state this is consistent with the explanation that such a phase shift can occur if the symmetry of the electronic state switches [12,16].

For double capture at most only a very weak interference structure was found. Due to this very small (or zero) visibility for this process it is not possible to gain new insight from these data into the phase shift in the interference pattern that was observed in some cases, including our data on vibrational dissociation. So far, no systematic pattern has emerged that would suggest under what condition a phase shift may be present or not (apart from a switch in electronic symmetry). A phase shift has not been reported yet for processes in which the molecule does not fragment. However, for processes which do involve fragmentation, phase shifts were reported even when no switch in the symmetry of the electronic state occurred [15,30], or no phase shift was found although a switch in symmetry did occur [11]. Therefore, it seems important to study two-center interference in molecular fragmentation processes in more detail. So far, to the best of our knowledge, a π phase shift was only clearly identified for fragmentation proceeding through a one-electron process [12,15,16,30]. Therefore, FDCS measurements for two-electron processes leading to fragmentation (like, e.g., double capture or double ionization) for fast projectiles would be particularly interesting. In this case, two-electron processes are usually dominated by a correlated single scattering process and a pronounced interference structure should be observable. A confirmation of a pattern linking a phase shift to one-electron fragmentation processes by such measurements could represent a major step towards a complete understanding of the phase angle in the two-center interference term.

[1] H. Ehrhardt, K. Jung, G. Knoth, and P. Schlemmer, Z. Phys. D **1**, 3 (1986).

[2] T. N. Rescigno, M. Baertschy, W. A. Issacs, and C. W. McCurdy, Science **286**, 2474 (1999).

[3] M. Schulz, R. Moshammer, D. Fischer, H. Kollmus, D. H. Madison, S. Jones, and J. Ullrich, Nature **422**, 48 (2003).

[4] M. Schulz and D. H. Madison, Int. J. Mod. Phys. A **21**, 3649 (2006).

[5] T. F. Tuan and E. Gerjuoy, Phys. Rev. **117**, 756 (1960).

[6] S. Cheng, C. L. Cocke, V. Frohne, E. Y. Kamber, J. H. McGuire, and Y. Wang, Phys. Rev. A **47**, 3923 (1993).

[7] N. Stolterfoht, B. Sulik, V. Hoffmann, B. Skogvall, J. Y. Chesnel, J. Rangama, F. Frèmont, D. Hennecart, A. Cassimi, X. Husson, A. L. Landers, J. A. Tanis, M. E. Galassi, and R. D. Rivarola, Phys. Rev. Lett. **87**, 023201 (2001).

[8] D. S. Milne-Brownlie, M. Foster, J. Gao, B. Lohmann, and D. H. Madison, Phys. Rev. Lett. **96**, 233201 (2006).

[9] D. Misra, U. Kadhane, Y. P. Singh, L. C. Tribedi, P. D. Fainstein, and P. Richard, Phys. Rev. Lett. **92**, 153201 (2004).

[10] E. M. Staicu Casagrande, A. Naja, F. Mezdari, A. Lahmam-Bennani, P. Bolognesi, B. Joulakian, O. Chuluunbaatar, O. Al-Hagan, D. H. Madison, D. V. Fursa, and I. Bray, J. Phys. B **41**, 025204 (2008).

[11] H. T. Schmidt, D. Fischer, Z. Berenyi, C. L. Cocke, M. Gudmundsson, N. Haag, H. A. B. Johansson, A. Källberg, S. B. Levin, P. Reinhed, U. Sassenberg, R. Schuch, A. Simonsson, K. Stöchkel, and H. Cederquist, Phys. Rev. Lett. **101**, 083201 (2008).

[12] L. Ph. H. Schmidt, S. Schössler, F. Afaneh, M. Schöffler, K. E. Stiebing, H. Schmidt-Böcking, and R. Dörner, Phys. Rev. Lett. **101**, 173202 (2008).

[13] J. S. Alexander, A. C. Laforge, A. Hasan, Z. S. Machavariani, M. F. Ciappina, R. D. Rivarola, D. H. Madison, and M. Schulz, Phys. Rev. A **78**, 060701(R) (2008).

[14] M. E. Galassi, R. D. Rivarola, and P. D. Fainstein, Phys. Rev. A **70**, 032721 (2004).

[15] A. Senftleben, T. Pflüger, X. Ren, O. Al-Hagan, B. Najjari, D. Madison, A. Dorn, and J. Ullrich, J. Phys. B **43**, 081002 (2010).

[16] S. F. Zhang, D. Fischer, M. Schulz, A. B. Voitkiv, A. Senftleben, A. Dorn, J. Ullrich, X. Ma, and R. Moshammer, Phys. Rev. Lett. **112**, 023201 (2014).

[17] K. N. Egodapitiya, S. Sharma, A. Hasan, A. C. Laforge, D. H. Madison, R. Moshammer, and M. Schulz, Phys. Rev. Lett. **106**, 153202 (2011).

[18] S. Sharma, A. Hasan, K. N. Egodapitiya, T. P. Arthanayaka, G. Sakhelashvili, and M. Schulz, Phys. Rev. A **86**, 022706 (2012).

[19] S. Sharma, T. P. Arthanayaka, A. Hasan, B. R. Lamichhane, J. Remolina, A. Smith, and M. Schulz, Phys. Rev. A **90**, 052710 (2014).

[20] T. P. Arthanayaka, S. Sharma, B. R. Lamichhane, A. Hasan, J. Remolina, S. Gurung, and M. Schulz, J. Phys. B **48**, 071001 (2015).

[21] J. M. Feagin and L. Hargreaves, Phys. Rev. A **88**, 032705 (2013).

[22] S. Sharma, T. P. Arthanayaka, A. Hasan, B. R. Lamichhane, J. Remolina, A. Smith, and M. Schulz, Phys. Rev. A **89**, 052703 (2014).

[23] T. P. Arthanayaka, S. Sharma, B. R. Lamichhane, A. Hasan, J. Remolina, S. Gurung, L. Sarkadi, and M. Schulz, J. Phys. B **48**, 175204 (2015).

[24] T. Arthanayaka, B. R. Lamichhane, A. Hasan, S. Gurung, J. Remolina, S. Borbély, F. Járai-Szabó, L. Nagy, and M. Schulz, J. Phys. B **49**, 13LT02 (2016).

[25] M. Schulz, in *Advances in Atomic, Molecular, and Optical Physics* Vol. 66, edited by E. Arimondo, C. C. Lin, and S. Yelin (Elsevier, Cambridge, MA, 2017), p. 508.

[26] X. Wang, K. Schneider, A. LaForge, A. Kelkar, M. Grieser, R. Moshammer, J. Ullrich, M. Schulz, and D. Fischer, J. Phys. B **45**, 211001 (2012).

[27] K. Schneider, M. Schulz, X. Wang, A. Kelkar, M. Grieser, C. Krantz, J. Ullrich, R. Moshammer, and D. Fischer, Phys. Rev. Lett. **110**, 113201 (2013).

[28] H. Gassert, O. Chuluunbaatar, M. Waitz, F. Trinter, H.-K. Kim, T. Bauer, A. Laucke, C. Müller, J. Voigtsberger, M. Weller, J. Rist, M. Pitzer, S. Zeller, T. Jahnke, L. Ph. H. Schmidt, J. B. Williams, S. A. Zaytsev, A. A. Bulychev, K. A. Kouzakov, H. Schmidt-Böcking, R. Dörner, Yu. V. Popov, and M. S. Schöffler, Phys. Rev. Lett. **116**, 073201 (2016).

[29] F. Navarrete, M. F. Ciappina, L. Sarkadi, and R. O. Barrachina Nucl. Instrum. Meth. B **408**, 165 (2017).

[30] B. R. Lamichhane, T. Arthanayaka, J. Remolina, A. Hasan, M. F. Ciappina, F. Navarrete, R. O. Barrachina, R. A. Lomsadze, and M. Schulz, Phys. Rev. Lett. **119**, 083402 (2017).

[31] H. F. Busnengo, S. E. Corchs, and R. D. Rivarola, Phys. Rev. A **56**, 1042 (1997).

[32] M. Dürr, B. Najjari, M. Schulz, A. Dorn, R. Moshammer, A. B. Voitkiv, and J. Ullrich, Phys. Rev. A **75**, 062708 (2007).

[33] I. Ben-Itzhak, V. Krishnamurthi, K. D. Carnes, H. Aliabadi, H. Knudsen, U. Mikkelsen, and B. D. Esry, J. Phys. B **29**, L21 (1996).

[34] A. K. Edwards, R. M. Wood, J. L. Davis, and R. L. Ezell, Phys. Rev. A **42**, 1367 (1990).

[35] A. K. Edwards and Q. Zheng, J. Phys. B **33**, 881 (2000).

[36] D. Misra, H. T. Schmidt, M. Gudmundsson, D. Fischer, N. Haag, H. A. B. Johansson, A. Källberg, B. Najjari, P. Reinhed, R. Schuch, M. Schöffler, A. Simonsson, A. B. Voitkiv, and H. Cederquist, Phys. Rev. Lett. **102**, 153201 (2009).